Submitted to the
XXXIII International Conference on High Energy Physics
July 26 - August 2, 2006, Moscow, Russia

Sessions: QCD hard interactions & Electroweak

Measurement of high-Q^2 charged current deep inelastic scattering cross sections with a longitudinally polarised electron beam at HERA

ZEUS Collaboration

Abstract

Measurements of the cross sections for charged current deep inelastic scattering in e^-p collisions with a longitudinally polarised electron beam are presented. The measurements are based on a data sample with an integrated luminosity of 122 pb^{-1} collected with the ZEUS detector at HERA in 2004 and 2005 at a centre-of-mass energy of 318 GeV. The total cross section is presented at positive and negative values of the longitudinal polarisation of the electron beam, with an estimate of the right-handed charged current cross section and a lower limit on the mass of a right-handed W boson. In addition, the single differential cross sections, $d\sigma/dQ^2$, $d\sigma/dx$ and $d\sigma/dy$, and the double differential cross section, $d^2\sigma/dxdQ^2$, are presented in the kinematic region $Q^2 > 200$ GeV^2. The measured cross sections are compared with the predictions of the Standard Model.

1 Introduction

Deep inelastic scattering (DIS) of leptons off nucleons has proved to be a key tool in the understanding of the structure of the proton and the form of the Standard Model (SM). The HERA *ep* collider has made possible the exploration of DIS at high values of negative four-momentum-transfer squared, Q^2. Using data taken in the years 1994-2000 the H1 and ZEUS collaborations have reported measurements of the cross sections for charged current (CC) DIS [1–12]. These measurements extend the kinematic region covered by fixed-target proton structure measurements [13–16] to higher Q^2.

The SM predicts that the cross section for charged current *ep* DIS should exhibit dependence on the longitudinal polarisation of the incoming lepton beam. The dependence is predicted to be linear with the cross section becoming zero for right-handed (left-handed) electron (positron) beams, due to the chiral nature of the weak interaction.

This paper presents measurements of the cross sections for e^-p CC DIS with a longitudinally polarised electron beam and an estimate of the cross section for right-handed e^-p CC DIS. The measurements are based on data samples collected with the ZEUS detector in 2004 and 2005 with integrated luminosities of 78.8 pb^{-1} and 42.7 pb^{-1} at mean luminosity weighted polarisations of -0.27 and +0.33, respectively. Figure 1 shows the luminosity collected as a function of the longitudinal polarisation of the electron beam. During this time HERA collided protons of energy 920 GeV with electrons of energy 27.5 GeV, yielding collisions at a centre-of-mass energy of 318 GeV. The measured cross sections are compared with the SM predictions and previous ZEUS measurements of e^+p CC DIS with a longitudinally polarised positron beam [17]. Similar results in e^+p CC DIS have recently been published by the H1 Collaboration [18].

2 Kinematic variables and cross sections

Inclusive deep inelastic lepton-proton scattering can be described in terms of the kinematic variables x, y and Q^2. The variable Q^2 is defined to be $Q^2 = -q^2 = -(k - k')^2$ where k and k' are the four-momenta of the incoming and scattered lepton, respectively. Bjorken x is defined by $x = Q^2/2P\cdot q$ where P is the four-momentum of the incoming proton. The variable y is defined by $y = P\cdot q/P\cdot k$. The variables x, y and Q^2 are related by $Q^2 = sxy$, where $s = 4E_eE_p$ is the square of the lepton-proton centre-of-mass energy (neglecting the masses of the incoming particles) and E_e and E_p are the energies of the incoming electron and proton, respectively.

The electroweak Born level cross section for the CC reaction, $e^-p \to \nu_e X$, with a longitudinally polarised electron beam (defined in Eqn. (1)), can be expressed at leading order in QCD as [19]

$$\frac{d^2\sigma^{\rm CC}(e^-p)}{dxdQ^2} = (1-P_e)\frac{G_F^2}{4\pi x}\left(\frac{M_W^2}{M_W^2+Q^2}\right)^2\left[Y_+F_2^{\rm CC}(x,Q^2)+Y_-xF_3^{\rm CC}(x,Q^2)\right],$$

where G_F is the Fermi constant, M_W is the mass of the W boson and $Y_\pm = 1 \pm (1-y)^2$. The structure functions $F_2^{\rm CC}$ and $xF_3^{\rm CC}$ for e^-p collisions may be written in terms of sums and differences of quark and anti-quark parton density functions (PDFs) as follows:

$$F_2^{\rm CC} = x[u(x,Q^2)+c(x,Q^2)+\bar{d}(x,Q^2)+\bar{s}(x,Q^2)],$$

$$xF_3^{\rm CC} = x[u(x,Q^2)+c(x,Q^2)-\bar{d}(x,Q^2)-\bar{s}(x,Q^2)],$$

where, for example, the PDF $u(x,Q^2)$ gives the number density of up quarks with momentum-fraction x at a given Q^2. The longitudinal polarisation of the electron beam, P_e, is defined as

$$P_e = \frac{N_R - N_L}{N_R + N_L}, \tag{1}$$

where N_R and N_L are the numbers of right and left-handed electrons in the beam.

The reduced cross section for the charged current reaction is defined as

$$\tilde{\sigma} = \left[\frac{G_F^2}{2\pi x}\left(\frac{M_W^2}{M_W^2+Q^2}\right)^2\right]^{-1}\frac{d^2\sigma^{\rm CC}}{dxdQ^2}.$$

ZEUS is a multipurpose detector, which is described in detail elsewhere [20]. Charged current events are characterised by a large missing transverse momentum, $P_{T,\rm miss}$, which is calculated as

$$P_{T,\rm miss}^2 = P_x^2 + P_y^2 = \left(\sum_i E_i\sin\theta_i\cos\phi_i\right)^2 + \left(\sum_i E_i\sin\theta_i\sin\phi_i\right)^2,$$

where the sums run over all calorimeter energy deposits E_i. The quantities θ_i and ϕ_i are the polar and azimuthal angles of the energy deposits as viewed from the interaction vertex[1]. The hadronic polar angle, γ_h, is defined by $\cos\gamma_h = (P_{T,\rm miss}^2 - \delta^2)/(P_{T,\rm miss}^2 + \delta^2)$, where $\delta = \sum(E_i - E_i\cos\theta_i) = \sum(E-P_z)_i$. In the naive Quark Parton Model, γ_h gives the scattering angle of the struck quark in the lab frame. The total transverse energy, E_T, is given by $E_T = \sum E_i\sin\theta_i$.

[1] The ZEUS coordinate system is a right-handed Cartesian system, with the Z axis pointing in the proton beam direction, referred to as the "forward direction", and the X axis pointing left towards the centre of HERA. The polar angle, θ, is measured with respect to the proton beam direction. The coordinate origin is at the nominal interaction point.

The ratio of the parallel, V_P, and antiparallel, V_{AP}, components of the hadronic transverse momentum can be used to distinguish CC DIS from photoproduction events. These variables are defined as

$$V_P = \sum_i \overrightarrow{P}_{T,i} \cdot \overrightarrow{n}_{P_{T,miss}} \quad \text{for} \quad \overrightarrow{P}_{T,i} \cdot \overrightarrow{n}_{P_{T,miss}} > 0,$$

$$V_{AP} = -\sum_i \overrightarrow{P}_{T,i} \cdot \overrightarrow{n}_{P_{T,miss}} \quad \text{for} \quad \overrightarrow{P}_{T,i} \cdot \overrightarrow{n}_{P_{T,miss}} < 0,$$

where the sums are performed over all calorimeter cells and $\overrightarrow{n}_{P_{T,miss}} = \overrightarrow{P}_{T,miss}/P_{T,miss}$.

The kinematic variables for charged current events were reconstructed from the measured $P_{T,\text{miss}}$ and δ using the Jacquet-Blondel method [21]. The estimators of y, Q^2 and x are: $y_{JB} = \delta/(2E_e)$, $Q^2_{JB} = P^2_{T,\text{miss}}/(1 - y_{JB})$ and $x_{JB} = Q^2_{JB}/(sy_{JB})$.

In the following, measurements of total cross sections, differential cross sections in x, y and Q^2 and reduced cross sections for CC DIS are presented. The cross section for right-handed CC DIS is estimated by performing a linear fit to measurements of the CC DIS total cross section as a function of longitudinal electron beam polarisation. From this estimate, a lower limit on the mass of a right-handed W boson is derived.

3 Monte Carlo simulation

Monte Carlo simulation (MC) was used to determine the efficiency for selecting events, the accuracy of kinematic reconstruction, to estimate the background rate and to deduce cross sections for the full kinematic region from the data. A sufficient number of events was generated to ensure that uncertainties from MC statistics are small. The MC samples were normalised to the total integrated luminosity of the data.

CC DIS signal events and NC DIS background events, including radiative effects, were simulated using the DJANGOH 1.3 [22] generator. The hadronic final state was simulated using the colour-dipole model of ARIADNE 4.10 [23] and, as a systematic check for the CC DIS events, the MEPS model of LEPTO 6.5 [24]. Both programs use the Lund string model of JETSET 7.4 [25] for the hadronisation. Photoproduction background was estimated using events simulated with HERWIG 5.9 [26]. Events simulated with GRAPE 1.1 [27] and EPVEC 1.0 [28] were used to estimate the background contribution from di-lepton and single W production, respectively.

4 Event selection

The following criteria were imposed to select CC DIS events and reject background.

- missing transverse momentum: $P_{T,\mathrm{miss}} > 12\,\mathrm{GeV}$ was required and, in addition, the missing transverse momentum excluding the calorimeter cells adjacent to the forward beam hole, $P'_{T,\mathrm{miss}}$, was required to exceed $10\,\mathrm{GeV}$;

- primary vertex: events were required to satisfy $|Z_{\mathrm{vtx}}| < 50$ cm. The Z coordinate of the ep interaction vertex, reconstructed using tracks in the central tracking detectors, was required to be in the centre of the detector. For events with an hadronic angle, γ_h, of less than $23°$ the vertex position was set to the nominal value of zero, and the $P_{T,\mathrm{miss}}$ and $P'_{T,\mathrm{miss}}$ thresholds increased to 14 and 12 GeV, respectively;

- rejection of photoproduction: for events with $\gamma_h > 23°$ and $P_{T,\mathrm{miss}} < 20\,\mathrm{GeV}$, $V_{AP}/V_P < 0.23$ was required and for events with $\gamma_h > 23°$ and $20 < P_{T,\mathrm{miss}} < 30\,\mathrm{GeV}$, $V_{AP}/V_P < 0.31$ was required. These requirements demanded an azimuthally collimated energy flow. In addition, for events with $\gamma_h > 23°$ it was required that the azimuthal angle between the missing transverse momentum measured by the tracks and that measured by the calorimeter was less than one radian for events with $P_{T,\mathrm{miss}} > 45\,\mathrm{GeV}$. This requirement was tightened to 0.5 radians for events with $P_{T,\mathrm{miss}} < 45\,\mathrm{GeV}$;

- rejection of NC DIS: NC DIS events with a poorly measured scattered electron or hadronic jet can have significant missing transverse momentum. Events with $\delta > 30\,\mathrm{GeV}$ and an isolated electromagnetic cluster in the calorimeter were rejected;

- rejection of non-ep background: interactions between the beams and residual gas in the beam pipe or upstream accelerator components can lead to events with significant missing transverse momentum, however for these interactions the arrival times of energy deposits in the calorimeter are inconsistent with the bunch crossing time. The arrival times were used to reject such events. Events caused by interactions with the residual gas were characterised by a large fraction of tracks not associated with the ep interaction vertex and such events were rejected. Muon finding algorithms based on tracking, calorimeter and muon chamber information were used to reject events caused by cosmic rays or muons in the beam halo;

- kinematic region: events were required to satisfy $Q^2_{\mathrm{JB}} > 200\,\mathrm{GeV}^2$ and $y_{\mathrm{JB}} < 0.9$, where Q^2_{JB} and y_{JB} are the Jaquet-Blondel estimators of Q^2 and y, respectively. These requirements restricted the event sample to a kinematic region where the resolution of the kinematic quantities is good and the background is small.

A total of 1228 data events satisfied all criteria in the positive-polarisation sample and 4221 events in the negative-polarisation sample. The background contamination was estimated to be typically less than 1%, but reached almost 5% in the lowest Q^2 bin of the positive polarisation sample. Figure 2 shows comparisons of data and MC distributions, where it can be seen that the MC gives a good description of the data.

5 Systematic uncertainties

The major sources of systematic uncertainty in the measured cross sections were the calorimeter energy scale and the uncertainty in the parton-shower scheme. The former was estimated by varying the energy scale of the calorimeter sections by ±1-2%, as outlined in [11, 12]. The resulting shifts in the cross sections were typically less than 10%, but increased to $\sim 30\%$ in the highest x bin of the single-differential cross-section measurement and $\sim 40\%$ in the highest x and Q^2 bins of the reduced cross section measurement. To estimate the sensitivity of the results to the details of the simulation of the hadronic final state, the LEPTO MEPS model was used instead of the ARIADNE model for calculating the acceptance corrections. The largest effects of $\sim 10\%$ were observed at low Q^2 and low x.

The systematic effects of the selection cuts were estimated by varying the threshold value of each selection cut independently by ±10%, which is a reasonable match to the resolution. The resulting shifts in the cross sections were typically within ±5%.

The uncertainty in the small contribution from photoproduction was estimated by fitting the V_{AP}/V_P distribution with a linear combination of the signal and background MC samples and allowing the normalisation of the photoproduction MC to vary. No cut on V_{AP}/V_P was applied for this check. The normalisation of the photoproduction MC was then varied by the uncertainty determined from the fit (±40%), which resulted in changes to the measured cross sections within ±5%.

The individual uncertainties were added in quadrature separately for the positive and negative deviations from the nominal cross section values to obtain the total systematic uncertainty.

The electron beam polarisation was measured using the HERA Compton polarimeters [29, 30]. The relative uncertainty in the measured polarisation was 5.0%. The relative uncertainty in the measured luminosity was 3.5%.

6 Results

The total cross section, corrected to the Born level in the electroweak interaction, for e^-p CC DIS in the kinematic region $Q^2 > 200\,\mathrm{GeV}^2$ was measured to be

$$\sigma^{\mathrm{CC}}(P_e = +0.33 \pm 0.02) = 46.7 \pm 1.3(\mathrm{stat.})^{+1.5}_{-1.3}(\mathrm{syst.})\ \mathrm{pb},$$

$$\sigma^{\mathrm{CC}}(P_e = -0.27 \pm 0.01) = 87.4 \pm 1.3(\mathrm{stat.})^{+2.6}_{-2.5}(\mathrm{syst.})\ \mathrm{pb},$$

where the systematic uncertainty does not include the contributions from the uncertainty on the luminosity measurement.

The total cross section is shown as a function of the longitudinal polarisation of the lepton beam in Fig. 3, including previous ZEUS measurements from both e^-p and e^+p data [11, 12, 17]. The data are compared to the SM predictions evaluated at next-to-leading-order in QCD using the ZEUS-JETS PDFs [31] which describe the data well.

A linear function was fitted to the three measured e^-p points as a function of the longitudinal polarisation of the electron beam. The result of this fit is shown in Fig. 4. The fit was extrapolated to $P_e = +1$ to estimate the right-handed CC DIS cross section, which gave

$$\sigma^{\mathrm{CC}}(P_e = +1) = 0.8 \pm 3.1(\mathrm{stat.}) \pm 5.0(\mathrm{syst.})\ \mathrm{pb},$$

where the contributions from the uncertainties on the luminosity and polarisation measurements and the effects of correlations between the uncertainties on the three measurements are all included in the systematic uncertainty. This value is consistent with the SM value of zero. From this estimate, and assuming that right-handed CC DIS would have the same coupling and propagator dependence as the SM CC DIS, a 95% confidence level lower limit on the mass of a right-handed W boson was extracted as

$$M_{W_R} > 180\,\mathrm{GeV}.$$

The single-differential cross-sections, $d\sigma/dQ^2$, $d\sigma/dx$ and $d\sigma/dy$ for CC DIS are shown in Fig. 5. A clear difference is observed between the measurements for positive and negative longitudinal polarisation, which is independent of the kinematic variables. The effects are well described by the SM evaluated using the ZEUS-JETS PDFs.

Figures 6 and 7 show the reduced cross sections for CC DIS for positively and negatively longitudinally polarised electron beams. The measurements are well described by the SM evaluated using the ZEUS-JETS PDFs, demonstrating a good agreement across the whole kinematic range of this measurement.

7 Summary

The cross sections for CC DIS in e^-p collisions with longitudinally polarised electron beams have been measured. The measurements are based on data with an integrated luminosity of $122\,\mathrm{pb}^{-1}$ collected with the ZEUS detector in 2004 and 2005 at a centre-of-mass energy of 318 GeV. The total cross section is presented at positive and negative values of the longitudinal polarisation of the electron beam, with an estimate of the right-handed CC DIS cross section and a limit on the mass of a right-handed W boson. In addition, single differential and reduced cross sections are presented in the kinematic region $Q^2 > 200\ \mathrm{GeV}^2$. The measured cross sections are well described by the predictions of the SM.

References

[1] H1 Coll., T. Ahmed et al., Phys. Lett. **B 324**, 241 (1994).

[2] H1 Coll., S. Aid et al., Z. Phys. **C 67**, 565 (1995).

[3] H1 Coll., S. Aid et al., Phys. Lett. **B 379**, 319 (1996).

[4] H1 Coll., C. Adloff et al., Eur. Phys. J. **C 13**, 609 (2000).

[5] H1 Coll., C. Adloff et al., Eur. Phys. J. **C 19**, 269 (2001).

[6] H1 Coll., C. Adloff et al., Eur. Phys. J. **C 21**, 33 (2001).

[7] H1 Coll., C. Adloff et al., Eur. Phys. J. **C 30**, 1 (2003).

[8] ZEUS Coll., M. Derrick et al., Phys. Rev. Lett. **75**, 1006 (1995).

[9] ZEUS Coll., M. Derrick et al., Z. Phys. **C 72**, 47 (1996).

[10] ZEUS Coll., J. Breitweg et al., Eur. Phys. J. **C 12**, 411 (2000). Erratum in Eur. Phys. J. **C 27**, 305 (2003).

[11] ZEUS Coll., S. Chekanov et al., Phys. Lett. **B 539**, 197 (2002). Erratum in Phys. Lett. **B 552**, 308 (2003).

[12] ZEUS Coll., S. Chekanov et al., Eur. Phys. J. **C 32**, 1 (2003).

[13] CDHS Coll., H. Abramowicz et al., Z. Phys. **C 25**, 29 (1984).

[14] CDHSW Coll., J.P. Berge et al., Z. Phys. **C 49**, 187 (1991).

[15] CCFR Coll., E. Oltman et al., Z. Phys. **C 53**, 51 (1992).

[16] BEBC Coll., G.T. Jones et al., Z. Phys. **C 62**, 575 (1994).

[17] ZEUS Coll., S. Chekanov et al., Preprint hep-ex/0602026, 2006. Accepted by Phys. Lett. B.

[18] H1 Coll., A. Aktas et al., Phys. Lett. **B 634**, 173 (2006).

[19] R.J. Cashmore et al., *Proc. the Workshop on Future Physics at HERA*, G. Ingelman, A. De Roeck and R. Klanner (eds.), Vol. 1, p. 163. DESY, Hamburg, Germany (1996).

[20] ZEUS Coll., U. Holm (ed.), *The ZEUS Detector*. Status Report (unpublished), DESY (1993), available on `http://www-zeus.desy.de/bluebook/bluebook.html`.

[21] F. Jacquet and A. Blondel, *Proceedings of the Study for an ep Facility for Europe*, U. Amaldi (ed.), p. 391. Hamburg, Germany (1979). Also in preprint DESY 79/48.

[22] G.A. Schuler and H. Spiesberger, *Proc. Workshop on Physics at HERA*, W. Buchmüller and G. Ingelman (eds.), Vol. 3, p. 1419. Hamburg, Germany, DESY

(1991);
H. Spiesberger, HERACLES *and* DJANGOH*: Event Generation for ep Interactions at HERA Including Radiative Processes*, 1998, available on
`http://www.desy.de/~hspiesb/djangoh.html`.

[23] L. Lönnblad, Comp. Phys. Comm. **71**, 15 (1992).

[24] G. Ingelman, A. Edin and J. Rathsman, Comp. Phys. Comm. **101**, 108 (1997).

[25] T. Sjöstrand, Comp. Phys. Comm. **39**, 347 (1986);
T. Sjöstrand and M. Bengtsson, Comp. Phys. Comm. **43**, 367 (1987);
T. Sjöstrand, Comp. Phys. Comm. **82**, 74 (1994).

[26] G. Marchesini et al., Comp. Phys. Comm. **67**, 465 (1992).

[27] T. Abe, Comp. Phys. Comm. **136**, 126 (2001).

[28] U. Baur, J.A.M. Vermaseren and D. Zeppenfeld, Nucl. Phys. **B 375**, 3 (1992).

[29] M. Beckmann et al., Nucl. Inst. Meth. **A 479**, 334 (2002).

[30] D.P. Barber et al., Nucl. Inst. Meth. **A 329**, 79 (1993).

[31] ZEUS Coll., S. Chekanov et al., Eur. Phys. J. **C 42**, 1 (2005).

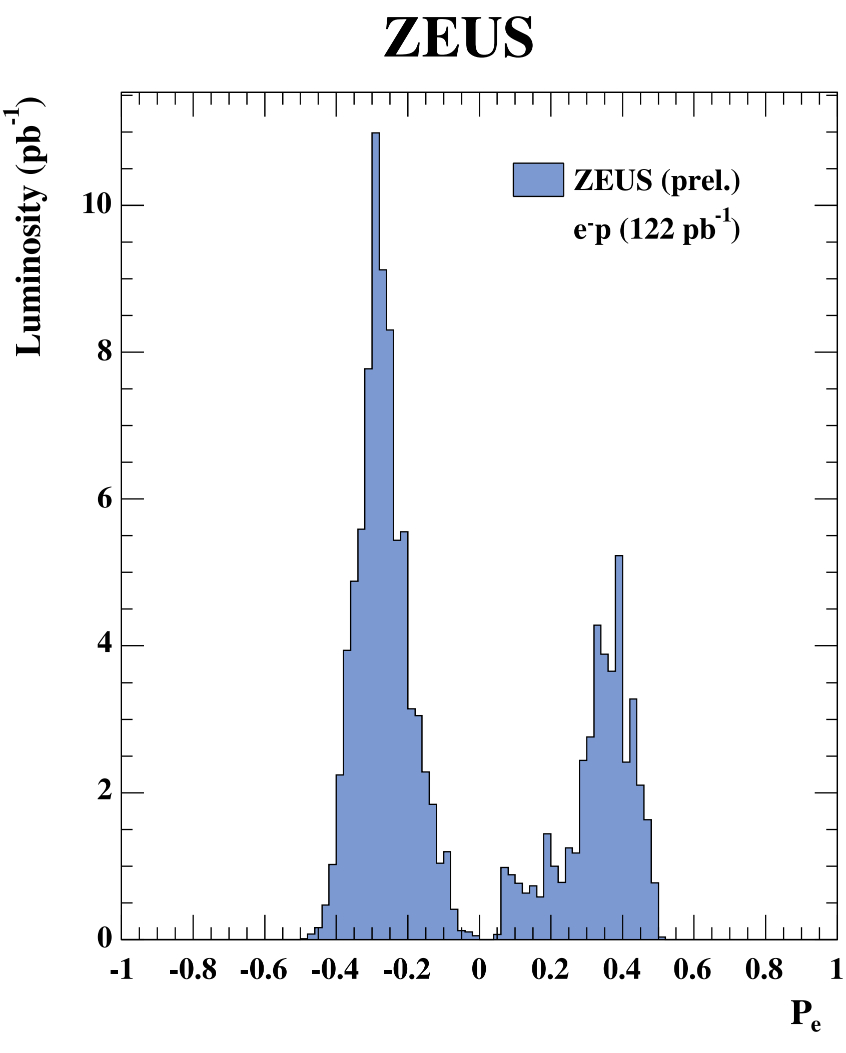

Figure 1: *The integrated luminosity collected as a function of the longitudinal polarisation of the electron beam.*

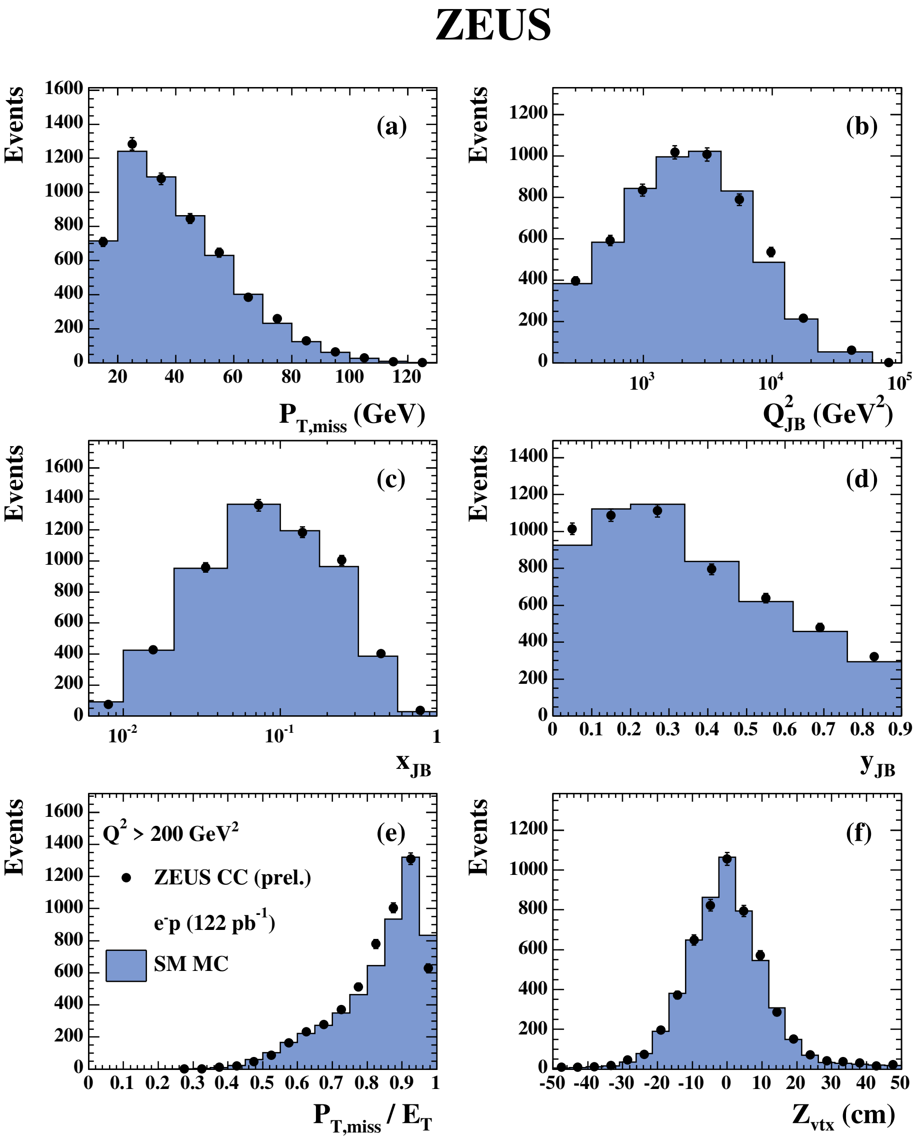

Figure 2: *Comparison of the final e^-p CC data sample with the expectations of the Monte Carlo simulation described in the text. The distributions of (a) missing transverse momentum, $P_{T,\mathrm{miss}}$, (b) Q^2_{JB}, (c) x_{JB}, (d) y_{JB}, (e) $P_{T,\mathrm{miss}}/E_T$ and (f) the Z coordinate of the event vertex, Z_{vtx}, are shown.*

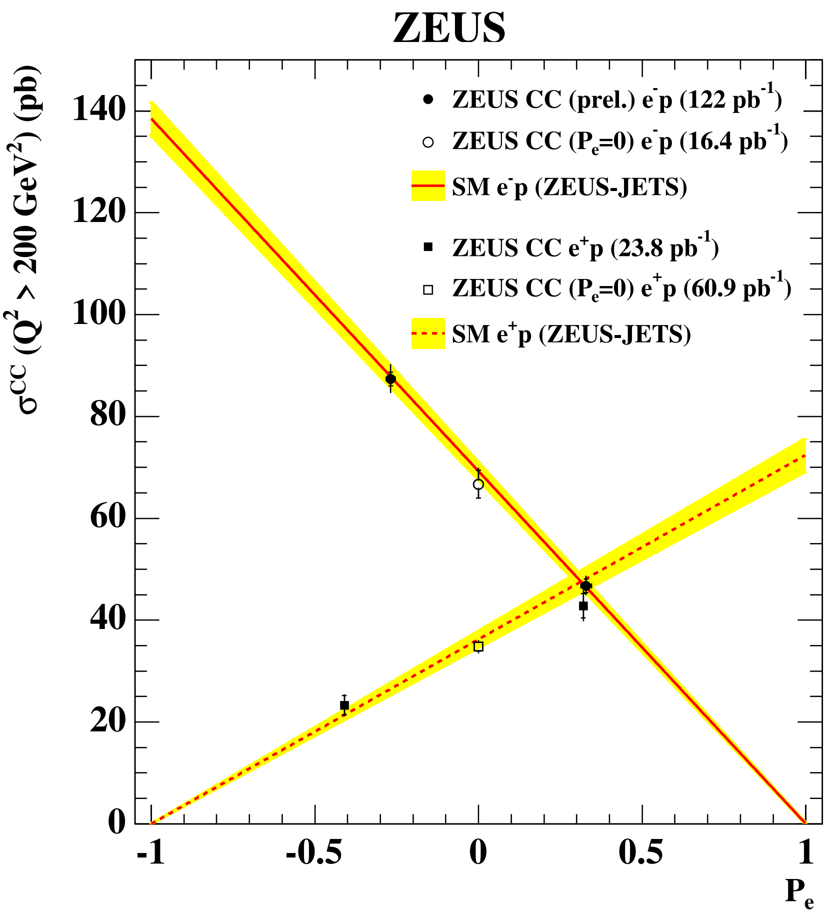

Figure 3: *The total cross sections for e^-p and e^+p CC DIS as a function of the longitudinal polarisation of the lepton beam. The lines show the predictions of the SM evaluated using the ZEUS-JETS PDFs.*

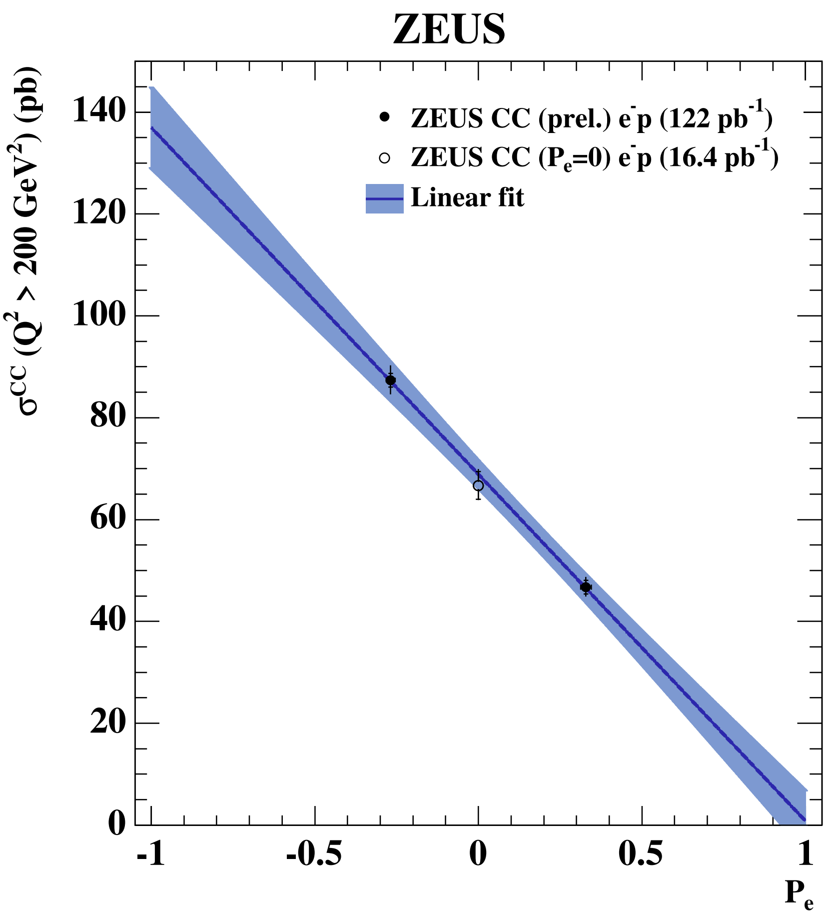

Figure 4: *The total cross section for e^-p CC DIS as a function of the longitudinal polarisation of the electron beam. The line shows the result of a linear fit performed to the three measured points and the shaded area shows the combined statistical and systematic uncertainty on the fit.*

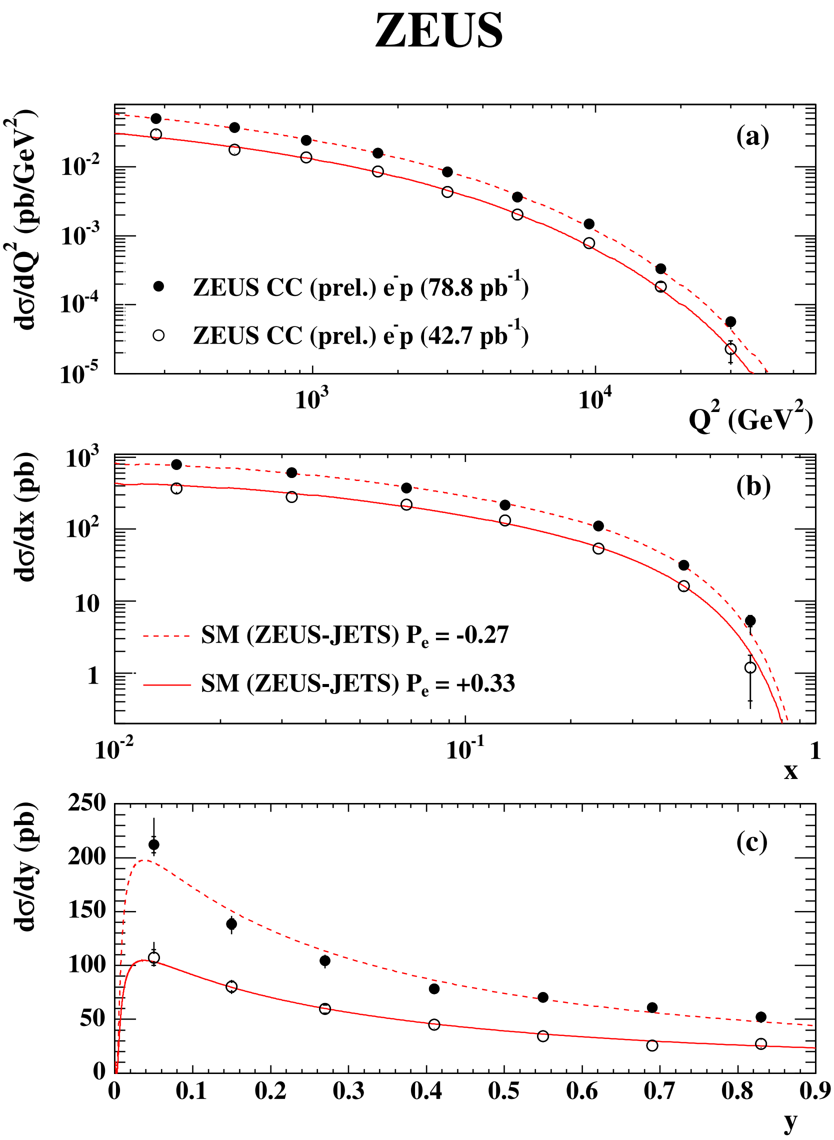

Figure 5: *The e^-p CC DIS cross-sections (a) $d\sigma/dQ^2$, (b) $d\sigma/dx$ and (c) $d\sigma/dy$. The closed (open) circles represent data points for the negative (positive) polarisation measurements and the curves show the predictions of the SM evaluated using the ZEUS-JETS PDFs.*

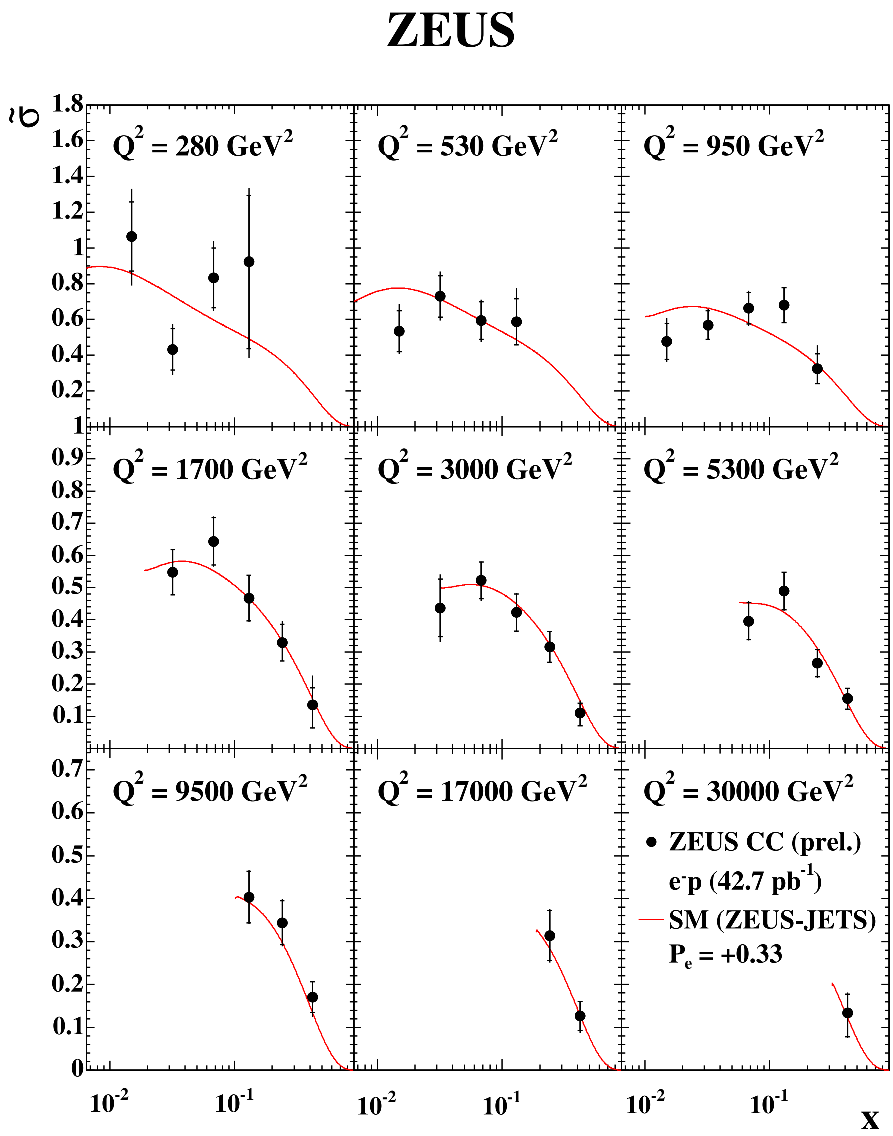

Figure 6: *The e^-p CC DIS reduced cross section plotted as a function of x in bins of fixed Q^2. The circles represent the data points for the positive polarisation measurements and the curves show the predictions of the SM evaluated using the ZEUS-JETS PDFs.*

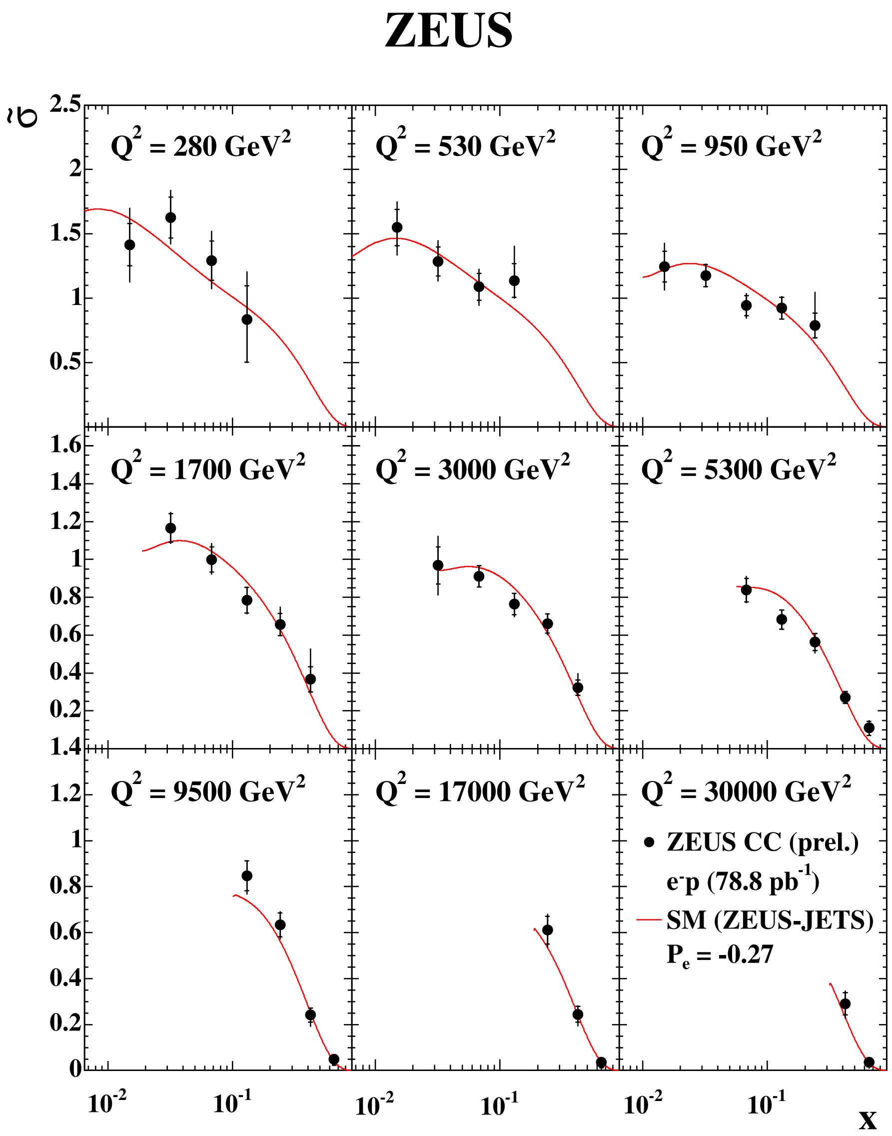

Figure 7: *The $e^{-}p$ CC DIS reduced cross section plotted as a function of x in bins of fixed Q^2. The circles represent the data points for the negative polarisation measurements and the curves show the predictions of the SM evaluated using the ZEUS-JETS PDFs.*